Polym. Bull. (2018) 75:149–165
https://doi.org/10.1007/s00289-017-2021-3

ORIGINAL PAPER

Polythiourethane microcapsules as novel self-healing systems for epoxy coatings

Tomasz Szmechtyk[1] · **Natalia Sienkiewicz**[1] · **Krzysztof Strzelec**[1]

Received: 2 February 2017 / Revised: 29 March 2017 / Accepted: 8 April 2017 /
Published online: 19 April 2017

Abstract A novel group of microcapsule-based self-healing systems for epoxy coatings was developed. Microcapsules with polythiourethane shell wall were synthesized via interfacial polymerization from selected diisocyanates and thiols and dispersed in epoxy matrix. The obtained composites were tested for their self-healing efficiency using three-point bending test (TPBT) and scratch test. Two sets of each composite samples as well as reference (neat diglycidyl ether of bisphenol A epoxy with polyamine adduct hardener) were tested with TPBT using two methods. Standard method according to ISO 178 was applied for the first set and custom method with pre-bending with 20 N force and standard TPBT after 24 h of self-healing—for the second set. Pre-bending was applied to obtain microcracks (without sample cracking) for internal self-healing process occurrence. Scratch test allowed to evaluate self-healing efficiency at composite surface and chemical resistance of samples. FT-IR spectroscopy was conducted to confirm occurrence of self-healing process based on polyurethane secondary network forming.

Keywords Self-healing · Microcapsules · Epoxy coating · Polythiourethanes · Polyurethanes

Introduction

Crack propagation and material damage during service are common problems for coatings made of epoxy resins. Solutions which have to meet these limitations are self-healing systems (S-HS). The simplest and the least expensive S-HS are microcontainers (microcapsules and hollow fibers) with healing agent inside,

✉ Tomasz Szmechtyk
tomaszszmechtyk@gmail.com

[1] Faculty of Chemistry, Institute of Polymer and Dye Technology, Lodz University of Technology, Stefanowskiego 12/16, 90-924 Lodz, Poland

dispersed in polymer matrix. Microcapsules are also more versatile option, because of wider spectrum and ease of synthesis methods. In both cases, self-healing process occurs when microcracks are propagating and shell wall of microcontainer ruptures. Consequently, liquid healing agent is released to polymer matrix and polymerizes forming secondary polymer matrix, which binds separated surfaces of microcracks.

First application of microcontainers as S-HS was in 1996—hollow glass fibers were filled with two-component epoxy glue [1]. Another solution was proposed by White et al. [2]. Urea–formaldehyde microcapsules containing dicyclopentadiene (DCPD) were dispersed in polymer matrix with Grubbs catalyst, which enabled ring-opening metathesis polymerization of DCPD released during crack propagation. Current, second generation of microcapsule-based S-HS focused on one-part and catalyst-free solutions, which were able to work in harsh environment, like water-reactive diisocyanates in polyurethane microcapsules [3]. The concept of this system was similar to first-generation self-healing mechanism. The difference is that self-healing after crack propagation is caused by isocyanate healing agent reactivity without the presence of catalyst (Fig. 1).

Reactivity of the healing agents is also a drawback, which could result in undesirable release and polymerization without crack healing. To avoid it, appropriate microcapsule shell wall is needed. Selection of shell wall with good mechanical properties is also important, because of particle dispersion in polymer matrix without significant loss of healing agent [4]. Wider spectrum of healing chemistries forced development of different microcapsule shell walls and methods of their synthesis [5–7]. Most common materials used for shell wall are polyureas [8–10], polyurethanes [3, 11, 12], melamine–formaldehyde [13–15] and urea–formaldehyde [2, 16, 17]. They can be obtained using different methods like in situ polymerization [2, 13–19], interfacial polymerization [3, 8–12, 20, 21], Pickering emulsion [22–24], microemulsion polymerization [25, 26], solvent evaporation/

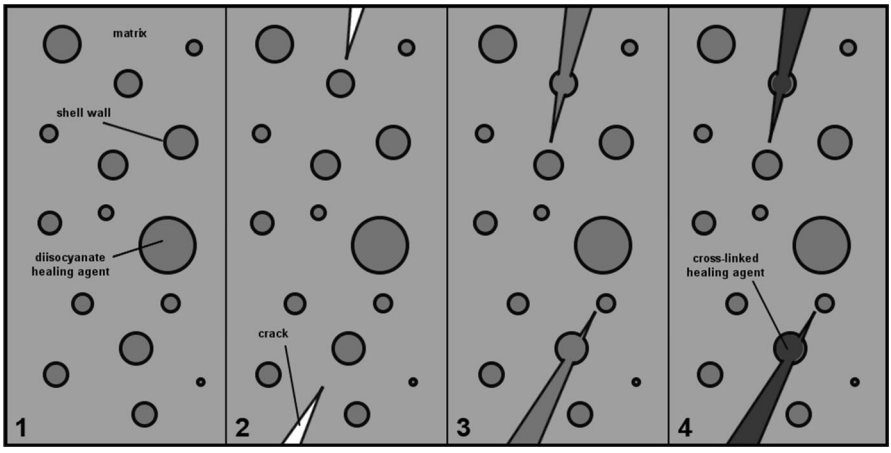

Fig. 1 Schematic of second-generation self-healing process: (*1*) coating with microcapsules before microcrack propagation, (*2*) microcracks occur, (*3*) microcapsules rupture and healing agent fills crack area, (*4*) healing agent reacts with water from environment and functional groups from matrix

extraction [27, 28] or sol–gel reaction [29, 30]. This variety of solutions entails much more self-healing mechanisms, which do not result only from aforementioned parameters. Current research focuses on modification of microcapsules to improve self-healing process. Di Credico et al. [31] tuned thickness of shell wall through diverse ingredients and process parameters. Other studies explored potential of multilayer microcapsules [23]: two healing agents in matrix [8, 9] or both solutions [22].

In this study, we present preliminary work on new S-HS for epoxy coatings and focus on influence of shell wall structure on self-healing mechanism. We selected polythiourethane (PTUR) as external shell material, because of thiourethane group reactivity with epoxy ring, which was reported in previous research [32, 33] and may improve adhesion between microcapsules and epoxy matrix. According to our knowledge, the only report that describes PTUR as shell material shows microcapsules obtained using Pickering emulsion [22] although, external shell layer of poly(glycidyl methacrylate) particles separates internal PTUR layer from epoxy matrix and there is no interaction between them.

Experimental

Materials

Isophorone diisocyanate (IPDI), hexamethylene diisocyanate (HDI), chlorobenzene, 3,6-dioxa-1,8-octanedithiol (DODT), trimethylolpropane tris(3-mercaptopropionate) (TTMP), pentaerythritol tetrakis(3-mercaptopropionate) (PETMP), dimethyl sulfoxide (DMSO), tetrahydrofuran (THF), potassium hydroxide (KOH), sulfuric acid (H_2SO_4) and 2,4,6-tris(dimethylaminomethyl)phenol (DMP-30) were obtained from Sigma-Aldrich. Epidian 5 epoxy resin (diglycidyl ether of bisphenol A with epoxide number of 0.487 and viscosity 23.9 Ns/m^2 at 25 °C.) with ET hardener (triethylenetetramine adduct with amine number 700–900 mg KOH/g, viscosity 200–300 mPa s and density 1.02–1.05 g/cm^3 [34]) were obtained from Organika-Sarzyna Inc. (Poland).

Synthesis of thiourethane prepolymer with reactive isocyanate groups

Thiourethane prepolymer (p-TUR) with reactive isocyanate groups was synthesized through reaction of DODT with HDI. Molar ratio [NCO]/[SH] = 2. 20.17 g (0.12 mol) of HDI was slowly added to 50 ml flask with stirring 11.2 g (0.06 mol) of DODT. The mixture was heated to 130 °C in oil bath and stirred for 1 h. Then the mixture was stirred for additional 3 h without heating. Obtained p-TUR was white and viscous paste, which was stored in 4 °C to avoid further polymerization.

Synthesis of IPDI filled polythiourethane microcapsules

Polythiourethane microcapsules (PTURmcaps) were prepared by two methods: with p-TUR (method 1) and without it (method 2). Microencapsulation via interfacial

polymerization based on Yang et al. recipe [3] was used in both methods. Lack of p-TUR in method 2 can cause formation of polyurea (PU) internal sub-layer.

Method 1 4.50 g of gum arabic was dissolved in 30 ml of deionized water and stirred for 3 h. 1 g of p-TUR was dissolved in 1.33 g (0.012 mol) of chlorobenzene at 50 °C. After obtaining clear solution of p-TUR 3.15 g (0.014 mol) of isophorone diisocyanate was added dropwise with stirring. The mixture was slowly added to 10 ml of gum arabic solution, heated to 50 °C and stirred (1000 rpm). Appropriate amount of thiol chain extender [DODT—2.13 g (0.012 mol); TTMP—3.15 g (0.008 mol); PETMP—2.82 g (0.006 mol)] was added and temperature of mixture was increased to 60 °C. After 1 h mixture was stirred without heating for additional 1 h to avoid agglomeration of microcapsules. Suspension of microcapsules was centrifuged and dried at 40 °C for 24 h to remove water.

Method 2 7.66 g (0.034 mol) of isophorone diisocyanate was mixed with 2.99 g (0.027 mol) of chlorobenzene at ambient temperature. Obtained mixture was slowly added to 15 ml of the gum arabic solution, heated to 50 °C and stirred with rotation rate of 1000 rpm. Appropriate amount of thiol chain extender [TTMP—3.15 g (0.008 mol); PETMP—2.82 g (0.006 mol)] was added. After 1 h mixture was stirred without heating for additional 1 h to avoid agglomeration of microcapsules. Suspension of microcapsules was centrifuged and dried at 40 °C for 24 h to remove water.

Preparation of epoxy composites

Obtained PTURmcaps were gently dispersed for 15 min with two-bladed glass propeller (powered by an electric motor) in Epidian 5 epoxy resin heated up to 40 °C. Composition was cured with ET hardener at room temperature. DMP-30 was used in one of the compositions as catalyst improving reactions between thiourethane and epoxy groups. In Table 1 seven various composites with five types of PTUR shell walls, different amount of microcapsules and presence of DMP-30 are listed.

Table 1 List of tested composites

No.	Composite name (type of shell wall/amount of microcapsules/additives)	Amount of components (phr)			
		Epidian 5	ET	PTURmcaps	DMP-30
1	p-TUR-DODT/18	100	18	18	0
2	p-TUR-TTMP/18	100	18	18	0
3	p-TUR-PETMP/18	100	18	18	0
4	IPDI-TTMP/18	100	18	18	0
5	IPDI-PETMP/18	100	18	18	0
6	IPDI-PETMP/30	100	18	30	0
7	IPDI-PETMP/30/DMP	100	18	30	1

phr parts by weight per 100 parts of epoxy resin

Optical microscopy

Optical microscopy was performed on a Leica MZ6 microscope. Obtained p-TURDODT microcapsules after centrifugation were placed on tefloned fabric and observed to investigate their morphology.

Atomic force microscopy (AFM)

AFM images were taken using Metrology Series 2000 (Molecular Imaging, USA) with tapping frequency 340 kHz. Selected images were also transformed into 3D surface maps.

Three-point bending test

Three-point bending test was conducted using Zwick/Roell 1435 universal testing machine (Germany) at room temperature, according to PN-EN ISO 178:2010 [35]. Unnotched rectangular specimens ($80 \times 10 \times 4$ mm^3) were bent with testing speed 2 mm/min. First set of all composites and hardened neat Epidian 5 as reference sample were tested sixfold using standard method. Obtained flexural stress at break (σ_{fB}) results and flexural modulus (E_f) for each composite were expressed as a mean value. Second set of all composites and reference were also tested sixfold using custom method (based on method proposed by Prajer et al. [36]) with pre-bending with 20 N force and standard test after 24 h. Pre-bending was applied to obtain microcracks (without sample cracking) and induce internal self-healing, which occurred at room temperature. Obtained flexural stress at break (σ_{fB}) and flexural modulus (E_f) results were also expressed as a mean value and compared to standard method results to quantify self-healing efficiency.

Fourier transform infrared (FT-IR) analysis

The FT-IR spectra were obtained by using Nicolet 6700 FT-IR spectrophotometer (Thermo Scientific, USA) equipped with a diamond crystal in an air atmosphere, at room temperature in a range of 400–4000 cm^{-1}. Spectra of each composite were taken before and after three-point bending test using ATR-mode with 32-scan signal. Spectra of virgin samples (before TPBT) and samples with self-healing effect (after TPBT) were taken three times, each from different region of sample to ensure self-healing evidence. The bands scales were normalized with OMNIC Spectra tool. Self-healing process was also confirmed by examination of 3360–3390 cm^{-1} shift.

Scratch test

Scratch test (according to method proposed by Huang et al. [9, 12]) was conducted to evaluate effect of microcapsules on chemical resistance and self-healing ability of composites (also in the presence of solvents and aqueous solutions). Samples were scratched (width of edge 0.58 ± 0.01 mm) and treated with selected solvents and

Table 2 Scratch test scales

Scale 1: self-healing efficiency	Point	Scale 2: chemical resistance	Point
No self-healing observed	0	No changes on surface	A
Low efficiency	1	Low level of changes	B
Average efficiency	2	Average level of changes	C
Good efficiency	3	High level of changes	D
Excellent efficiency	4	Severe damage on sample	E

solutions: water, 20% KOH aq., 20% H_2SO_4 aq., THF and DMSO. Also reference samples without treating were tested. All samples were covered with Petri dish to avoid evaporation of solvents and exclude the effect of atmospheric moisture. Optical micrographs were taken before treating and after 24 h exposure. Self-healing process occurred at room temperature. Changes on the surface and scratch area were evaluated visually (examples in Fig. 5) and scored on two five-point scales (Table 2).

Results and discussion

Synthesis and characterization of prepolymer and microcapsules

The synthesis of thiourethane prepolymer was achieved by reaction between isocyanate groups of HDI and thiol groups of DODT. HDI/DODT molar ratio 2:1 allowed to obtain prepolymer with isocyanate groups at chain ends (Scheme 1).

Prepolymer was used in method 1 to synthesize PTUR shell wall of microcapsules with DODT, TTMP and PETMP as chain extenders. Ratio of thiol groups to isocyanate groups from p-TUR was 1:1 with theoretical excess of isocyanate groups from IPDI for microcapsule content. Gum arabic worked as stabilizer together with p-TUR and both formed interfacial protecting layer to avoid

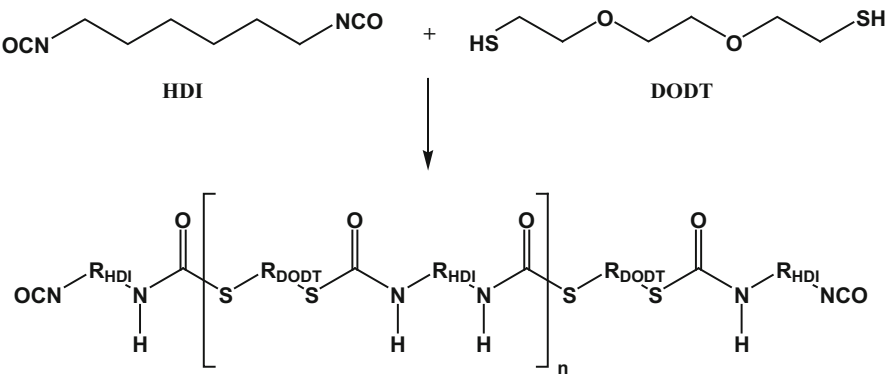

Scheme 1 Synthesis of thiourethane prepolymer (R_{HDI} HDI radical, R_{DODT} DODT radical)

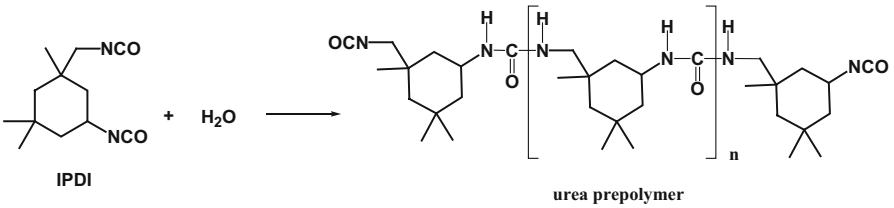

Scheme 2 Urea prepolymer formation from reaction of IPDI and water

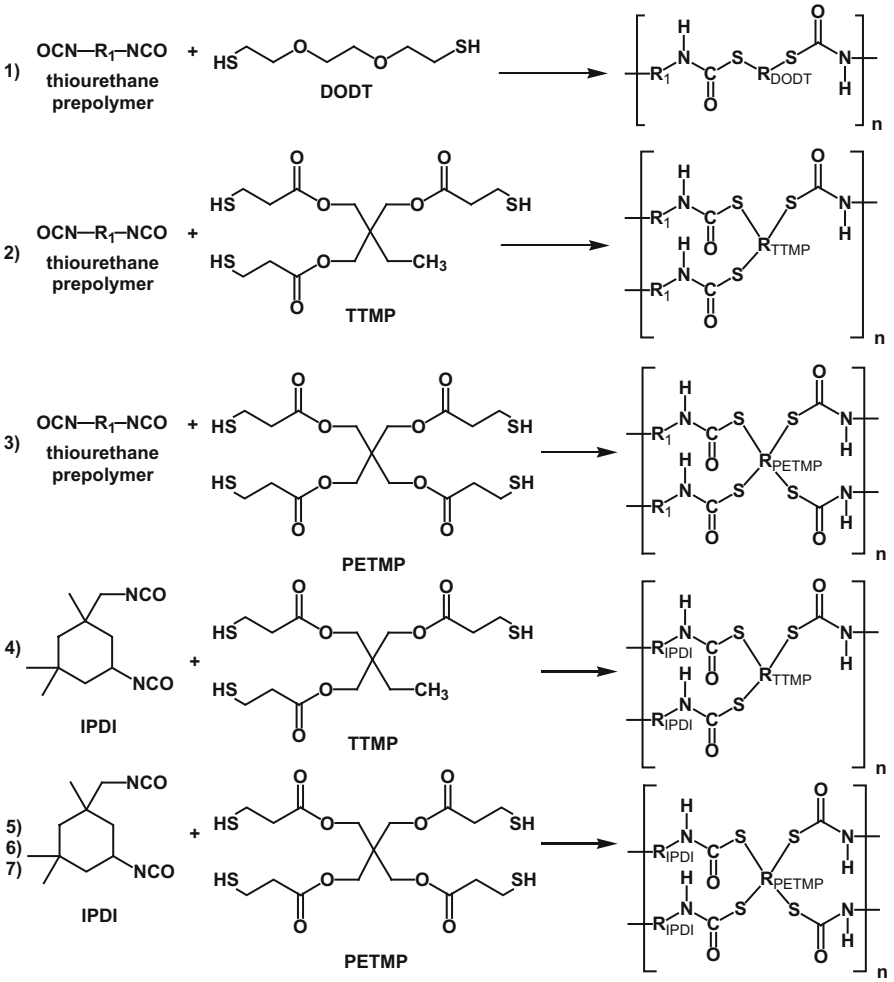

Scheme 3 Synthesis of all PTUR shell walls (R_1 p-TUR radical, R_{DODT} DODT radical, R_{TTMP} TTMP radical, R_{PETMP} PETMP radical, R_{IPDI} IPDI radical)

contact of reactive IPDI with water [31, 37]. In method 2 IPDI replaced thiourethane prepolymer as shell wall substrate. Consequently, lower stabilizing potential of pure gum arabic layer might cause initial reaction of IPDI with water and urea prepolymer (p-Urea) formation (Scheme 2).

Presence of p-Urea with gum arabic allowed to obtain interfacial protecting layer with stabilizing potential similar to p-TUR/gum arabic system and avoid further IPDI/water reaction [38]. The obtained microcapsules had polyurea internal sub-layer and external polythiourethane shell wall from TTMP or PETMP. Reactions of all PTUR shell walls are presented in Scheme 3.

Self-healing mechanism characterization

Microcrack propagation causes release of IPDI to epoxy matrix with free secondary hydroxyl groups. Presence of tertiary amines in cured epoxy matrix catalyze reaction between these hydroxyl groups and isocyanate groups from IPDI (Scheme 4). Also DMP-30 contains tertiary amine groups which support catalyst effect in composite 7 (highest self-healing efficiency in TPBT).

Optical microscopy

Optical microscopy images (Fig. 2) showed that PTURmcaps had spherical, ellipsoidal or quasi-spherical shape and their diameters varied from less than 0.1 to

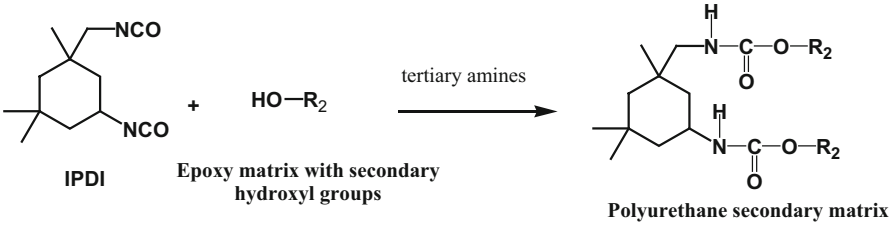

Scheme 4 Polyurethane secondary matrix forming Turing self-healing process (R_2 epoxy matrix)

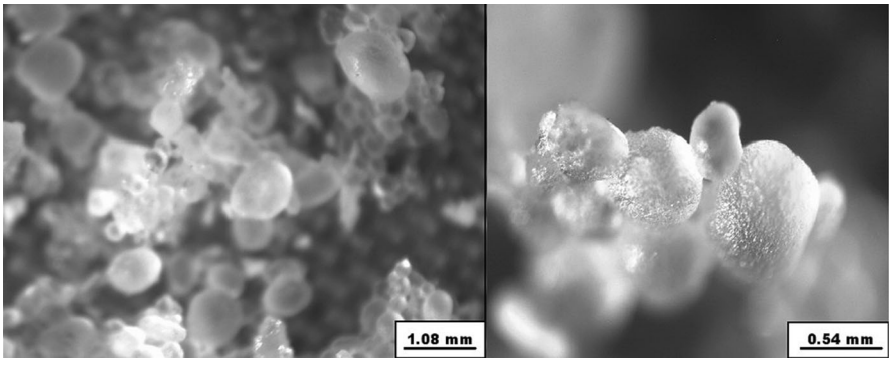

Fig. 2 Optical micrographs of p-TUR-DODT microcapsules

0.9 mm. Surface texture of external PTUR shell wall was uneven and rough. Microcapsules also showed tendency to form small clusters. Other types of microcapsules, even without prepolymer, looked very similar to presented one.

AFM

AFM images and 3D surface maps of IPDI-PETMP/30 composite (Fig. 3) confirm the presence of microcapsules at composite surface and small range of their diameters (2–20 μm). Also clustering effect is less pronounced in epoxy composite than between untreated microcapsules.

Three-point bending test

Mean values for both methods were compared to each other and calculated self-healing efficiencies after microcracking were presented in Table 3. Self-healing efficiency was calculated according to formula (1) proposed by Wool and O'Connor [39]:

$$E_{SH} = \frac{P_H}{P_V} \times 100\%, \quad (1)$$

where E_{SH} is self-healing efficiency, P_H is property of healed composite and P_V is property of virgin composite.

Three composites (p-TUR-TTMP/18, p-TUR-PETMP/18, IPDI-TTMP/18) did not reach 100% self-healing efficiency based on flexural stress at break, but this property was relatively higher in comparison with composites with IPDI-PETMP microcapsules. Similar tendency was observed for self-healing efficiencies based on flexural modulus. However, the presence of microcapsules reduced flexural rigidity of epoxy matrix, which resulted in lower flexural stress and modulus in all samples with PTURmcaps. As it might be expected, higher amount of PTURmcaps also resulted in better self-healing efficiency. Type of synthesis method also played role in self-healing efficiency. Composites with microcapsules containing p-TUR in shell wall provided lower efficiency than their counterparts without prepolymer. The best self-healing efficiency is shown by three systems with IPDI-PETMP microcapsules. IPDI-PETMP/18 composite comprises both high self-healing efficiency and satisfactory virgin properties.

FT-IR analysis

FT-IR spectra of reference sample and all composites with PTURmcaps (before and after three-point bending test) allowed to investigate changes in composite after self-healing. Spectra of reference sample and p-TUR-DODT/18 were presented in Fig. 4. Significant peaks of other composites with PTURmcaps were presented in Table 4 because of their resemblance to p-TUR-DODT/18.

All spectra of composites before self-healing have N–H and O–H stretching vibration broad band with highest peak around 3360 cm^{-1}, while all spectra of

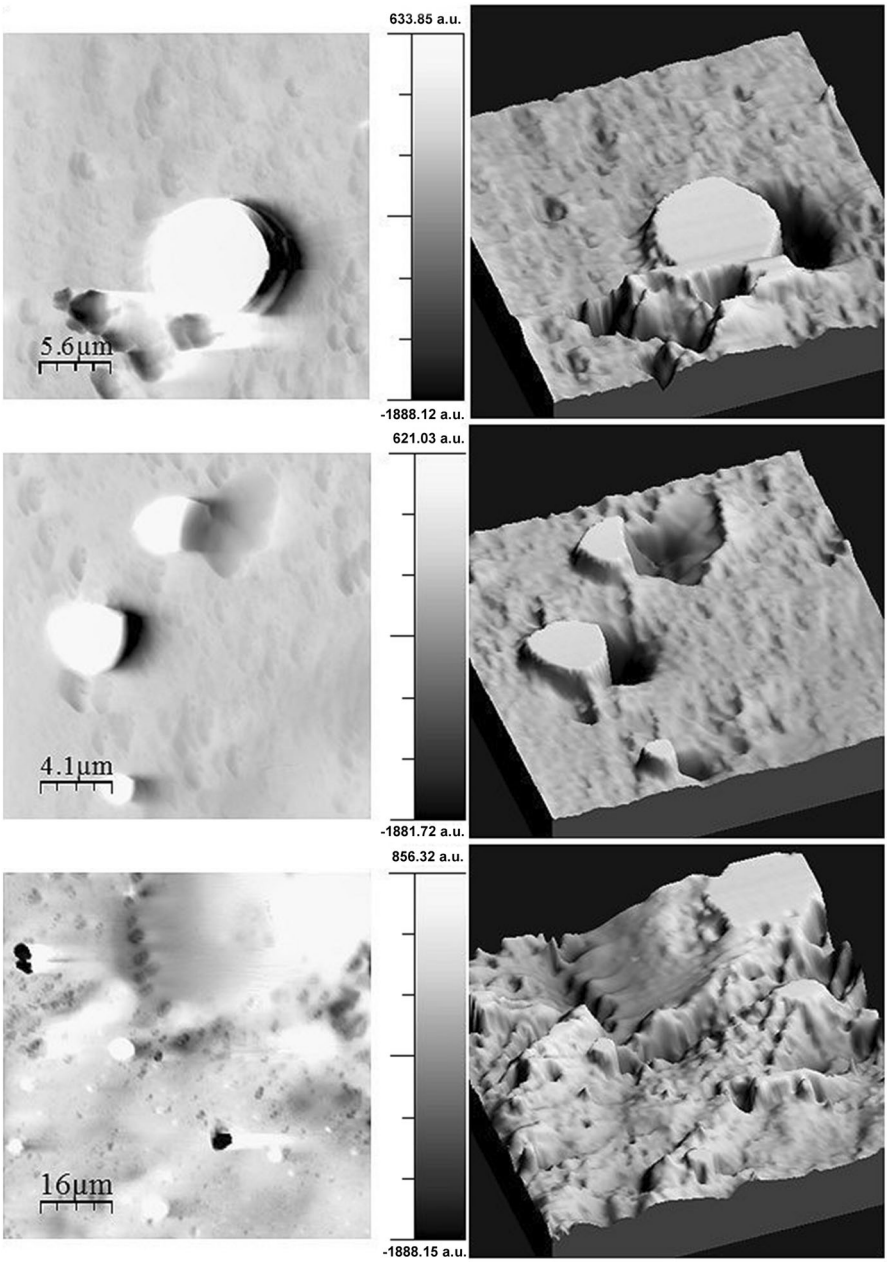

Fig. 3 AFM images (*left*) and 3D surface maps (*right*) of IPDI-PETMP/30 composite

composites after self-healing have this peak around 3390 cm^{-1}. This shift results from reduction of hydrogen bonding [40, 41] during self-healing process, which provides better cross-linking and aforementioned reduction. The higher intensity of

Table 3 Microcracks' self-healing efficiencies based on flexural stress at break and flexural modulus, measured using three-point bending test

No.	Composite name	Flexural stress at break (σ_{fB}) (MPa)		Flexural modulus (E_f) (MPa)		Microcracks self-healing efficiency (%)	
		Standard method (virgin)	Custom method (after 20 N pre-bending) (healed)	Standard method (virgin)	Custom method (after 20 N pre-bending) (healed)	σ_{fB}	E_f
0	Reference sample	43.7	–	2580	–	–	–
1	p-TUR-DODT/18	16.7	17.3	1980	2010	103.6	101.5
2	p-TUR-TTMP/18	22.0	14.3	1680	1580	65.0	94.0
3	p-TUR-PETMP/18	31.4	24.7	2280	2050	78.7	89.9
4	IPDI-TTMP/18	24.2	17.8	1840	1940	73.6	105.4
5	IPDI-PETMP/18	19.7	25.6	1630	2510	129.9	154.0
6	IPDI-PETMP/30	12.7	19.7	1290	1720	155.1	133.3
7	IPDI-PETMP/30/DMP	9.6	17.0	1230	2060	177.1	167.5

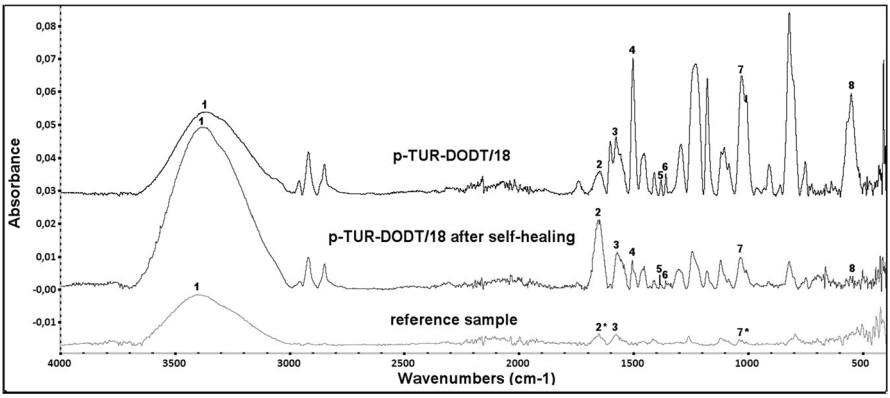

Fig. 4 FT-IR spectra of reference sample and p-TUR-DODT/18 (before and after self-healing): *1* N–H and O–H stretching; *2* C=O stretching (*aromatic ring overtone); *3* N–H bending; *4* NH–CO–S bending; *5* C–N axial stretching; *6* C–H bending (IPDI); *7* CH_2–S bending (*C–O stretching in alcohols); *8* C–S stretching

3390 cm^{-1} peaks after self-healing compared to 3360 cm^{-1} peaks is also effect of better cross-linking, more precisely polyurethane secondary network forming, which results from the conversion of isocyanate groups into urethane bonding. The lack of absorption band at 2600–2540 cm^{-1} (S–H stretching, thiol group) proved successful formation of PTUR shell wall with all amount of thiol chain extenders. Also isocyanate absorption bands around 2270–2260 cm^{-1} are not detected, even for composites before self-healing. This is justifiable for low microcapsule content and presence of PTUR shell wall around IPDI liquid core. The second reason for

Table 4 Significant FT-IR absorption peaks and their approximate assignments for all composites (*A*—after self-healing)

Composite number → Approximate assignment ↓	0	1	1A	2	2A	3	3A	4	4A	5	5A	6	6A	7	7A
N–H and O–H stretching (alcohols, amines, amides)	3396	3360	3388	3359	3393	3360	3393	3360	3397	3360	3397	3360	3396	3361	3390
C=O stretching, (amide groups: ureas, thiourethanes and urethanes); aromatic ring overtone*	1654*	1656	1656	1653	1650	1652	1656	1652	1648	1652	1648	1644	1651	1651	1657
		1652	1651			1641	1645	1644							1650
		1648													
		1644													
N–H bending (amines, thiourethanes and urethanes)	1580	1579	1579	1580	1575	1580	1580	1579	1581	1577	1578	1580	1574	1581	1574
							1574			1560	1544		1543	1556	
										1556					
–NH–CO–S– bending (thiourethanes); triazine compounds (isocyanurates)		1506	1508	1505	1510	1506	1507	1506	1506	1508	1509	1507	1508	1507	1507
C–N axial stretching (isocyanate group [42])		1383	1386	1384	1388	1384	1386	1383	1383	1390	1388	1382	1387	1383	1386
C–H bending in geminal dimethyl group (IPDI)		1361	1362	1361	1361	1361	1362	1361	1361		1362	1361	1362	1361	1362
–CH_2–S– bending [33]; C–O stretching (alcohols)*	1039*	1030	1034	1030	1037	1031	1029	1031	1027	1032	1038	1026	1038	1031	1028
	1028*														
C–S stretching		553	556	552	547	554	559	553	552	553	546	552	547	553	552
							546			547					

this absence is limited ATR penetration depth—only approximately 0.9 μm for a diamond crystal, which also shows strong absorption in wavenumber range between 1800 and 2650 cm^{-1}. Another characteristic peak at 1650 cm^{-1} is associated with C=O stretching vibration of secondary amide group in thiourethane and urethane moieties. This peak is also characteristic for C=O stretching vibration of tertiary amide group of urea. Significant increase of this peak is observed in all composites after self-healing, what confirms polyurethane secondary network forming. The presence of polythiourethanes and isocyanurates (as triazine derivatives) is confirmed by 1510–1500 cm^{-1} absorption band. Characteristic vibrations (C–N axial stretching) of isocyanate group are also observed at 1390–1380 cm^{-1} [42]. The presence of C–H bending vibration in geminal dimethyl group at 1360 cm^{-1} gives the proof of IPDI presence. Peaks around 1030 cm^{-1} (increased in all composites in comparison to reference sample alcohol C–O stretching) and around 550 cm^{-1} represent $–CH_2–S–$ bending [33] and C–S stretching in PTUR shell, respectively.

Scratch test

The obtained results (examples in Fig. 5) show show that the microcapsules content does not significantly affect the chemical resistance of composites to solvents and aqueous solutions (Table 5). Only chemical resistance to aqueous solutions of KOH and H_2SO_4 is lower in case of microcapsule-filled composites. However, all composites are still vulnerable to organic solvents, especially DMSO. The most effective self-healing process was obtained for p-TUR-TTMP/18 and p-TUR-PETMP/18 in the presence of water. Better self-healing efficiency is observed for

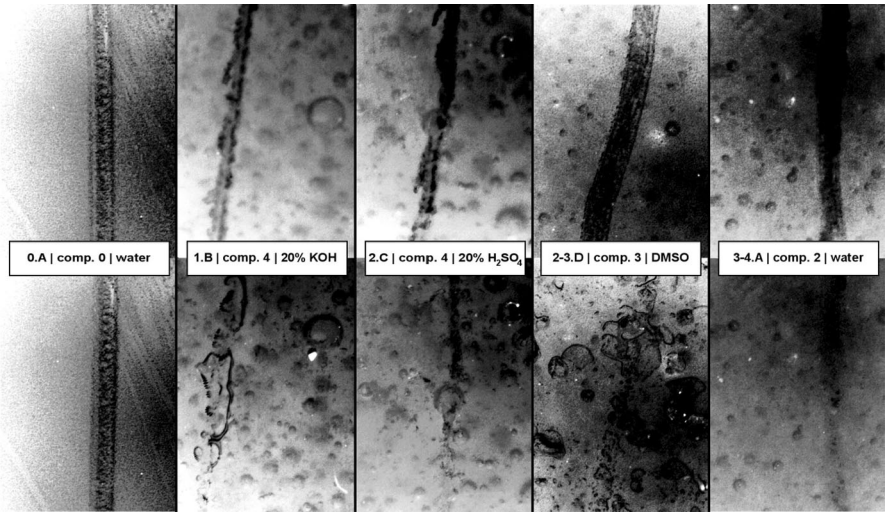

Fig. 5 Micrographs of samples before (*above description*) and after self-healing (*below description*) with all points observed on both scales. Description shows: classification on both scales, composite number and selected solvent/solution, respectively

Table 5 Evaluation of self-healing efficiency and chemical resistance after 24 h

No.	Composite name	Solvent/solution					
		–	Water	20% KOH aq.	20% H_2SO_4 aq.	THF	DMSO
0	Reference sample	0.A	0.A	0.A	0.A	0.B	0.C
1	p-TUR-DODT/18	1.A	2.A	2-3.A	3.B-C	3.B	3.B
2	p-TUR-TTMP/18	3.A	**3-4.A**	3.A-B	2.A-B	2-3.A-B	2.A-B
3	p-TUR-PETMP/18	2.A	**3-4.A**	2-3.A	2-3.A-B	2-3.B	2-3.D[a]
4	IPDI-TTMP/18	0-1.A	0-1.A	1.B	2.C	2.A-B	1-2.B
5	IPDI-PETMP/18	0-1.A	0-1.A	1.C-D	1.A	2.B	2.B-C
6	IPDI-PETMP/30	1-2.A	2.A	2-3.A	1-2.B	2-3.A-B	2.B-C
7	IPDI-PETMP/30/DMP	1-2.A	1-2.A	1.B-C	1-2.B	2.A-B	2.C

Bold values show best results

[a] High level of surface destruction impedes S–H efficiency evaluation

composites with prepolymer microcapsules, while content of microcapsules without p-TUR is not so effective.

Conclusions

Five types of microcapsules with PTUR shell wall were synthesized and applied in seven composites as self-healing systems. The obtained composites were tested for their surface self-healing efficiency (scratch test) and internal self-healing efficiency (three-point bending test). Also chemical resistance of the composites to selected solvents and solutions was examined. Overall, higher surface self-healing efficiency reveals composites with prepolymer microcapsules, contrary to internal self-healing efficiency, which is better provided by microcapsules without p-TUR. Healing process of microcracks in composites 1, 5, 6 and 7 furthermore strengthened these composites (over 100% self-healing efficiency). Comparison with other microcapsule-based self-healing systems for epoxy matrix shows that our self-healing system is competitive. Thiol-epoxy healing system in melamine–formaldehyde (MF) microcapsules from Yan et al. reached similar self-healing efficiency of 80–105% in the presence of amine catalyst [15]. In another system from Zhang and co-workers, MF microcapsules with functional glycidyl methacrylate achieved 75–90% E_{SH} without catalyst [14]. IPDI filled polyurethane and polyurea–formaldehyde microcapsules proposed by Di Credico et al. show more than 50% recovery (optical microscope evaluation) [31]. However, our goal was not only to obtain competitive self-healing system. Selection of similar systems, differing only in the structure of microcapsule PTUR shell wall allowed to investigate influence of these variables. As mentioned above, microcapsules with shell made of linear p-TUR oligomer worked better during scratch test, which examined self-healing ability of surface area. It probably results from oligomer chain flexibility, which provides better performance to scratch damage, but is less effective during internal crack

propagation. The only exception is composite with p-TUR-DODT microcapsules which performs well in both tests, probably due to the absence of crosslinking components—p-TUR and DODT are bifunctional and more organized structure results from chain entanglement. On the other hand, IPDI-based microcapsules with PU sub-layer work better during internal microcrack propagation, but are less effective when scratch damage occurs. It is presumably the result of their rigidity and greater brittleness, which helps IPDI-based microcapsules remain intact during primary epoxy curing and work properly, when microcrack propagation occurs.

FT-IR spectroscopy allowed to confirm self-healing process based on polyurethane secondary network forming. In conclusion, self-healing systems obtained in our preliminary work are suitable for epoxy coatings, especially in water and moisture environment. Future research will let us improve these self-healing systems' performance and investigate more thoroughly correlation between microcapsule structure and self-healing efficiency.

References

1. Dry C (1996) Procedures developed for self-repair of polymer matrix composite materials. Compos Struct 35:263–269. doi:10.1016/0263-8223(96)00033-5
2. White SR, Sottos NR, Geubelle PH, Moore JS, Kessler MR, Sriram SR, Brown EN, Viswanathan S (2001) Autonomic healing of polymer composites. Nature 409:794–797
3. Jinglei Y, Keller MW, Moore JS, White SR, Sottos NR (2008) Microencapsulation of isocyanates for self-healing polymers. Macromolecules 41:9650–9655. doi:10.1021/ma801718v
4. Keledi G, Hári J, Pukánszky B (2012) Polymer nanocomposites: structure, interaction, and functionality. Nanoscale 4:1919–1938. doi:10.1039/C2NR11442A
5. Hillewaere XKD, Du Prez FE (2015) Fifteen chemistries for autonomous external self-healing polymers and composites. Prog Polym Sci 49–50:121–153. doi:10.1016/j.progpolymsci.2015.04.004
6. Billiet S, Hillewaere XKD, Teixeira RFA, Du Prez FE (2013) Chemistry of crosslinking processes for self-healing polymers. Macromol Rapid Commun 34:290–309. doi:10.1002/marc.201200689
7. Zhu DY, Rong MZ, Zhang MQ (2014) Self-healing polymeric materials based on microencapsulated healing agents: from design to preparation. Prog Polym Sci 49–50:175–220. doi:10.1016/j.progpolymsci.2015.07.002
8. Hillewaere XKD, Teixeira RFA, Nguyen LTT, Ramos JA, Rahier H, Du Prez FE (2014) Autonomous self-healing of epoxy thermosets with thiol-isocyanate chemistry. Adv Funct Mater 24:5575–5583. doi:10.1002/adfm.201400580
9. Keller MW, Hampton K, McLaury B (2013) Self-healing of erosion damage in a polymer coating. Wear 307:218–225. doi:10.1016/j.wear.2013.09.005
10. Khun NW, Sun DW, Huang MX, Yang JL, Yue CY (2014) Wear resistant epoxy composites with diisocyanate-based self-healing functionality. Wear 313:19–28. doi:10.1016/j.wear.2014.02.011
11. Huang M, Yang J (2014) Salt spray and EIS studies on HDI microcapsule-based self-healing anticorrosive coatings. Prog Org Coatings 77:168–175. doi:10.1016/j.porgcoat.2013.09.002
12. Huang M, Yang J (2011) Facile microencapsulation of HDI for self-healing anticorrosion coatings. J Mater Chem 21:11123. doi:10.1039/c1jm10794a
13. Yuan YC, Rong MZ, Zhang MQ (2008) Preparation and characterization of microencapsulated polythiol. Polymer (Guildf) 49:2531–2541. doi:10.1016/j.polymer.2008.03.044

14. Meng LM, Yuan YC, Rong MZ, Zhang MQ (2010) A dual mechanism single-component self-healing strategy for polymers. J Mater Chem 20:6030–6038. doi:10.1039/C0JM00268B
15. Yan CY, Min ZR, Ming QZ, Chen J, Gui CY, Xue ML (2008) Self-healing polymeric materials using epoxy/mercaptan as the healant. Macromolecules 41:5197–5202. doi:10.1021/ma800028d
16. De La Paz Miguel M, Ollier R, Alvarez V, Vallo C (2016) Effect of the preparation method on the structure of linseed oil-filled poly(urea–formaldehyde) microcapsules. Prog Org Coatings 97:194–202. doi:10.1016/j.porgcoat.2016.04.026
17. Suryanarayana C, Rao KC, Kumar D (2008) Preparation and characterization of microcapsules containing linseed oil and its use in self-healing coatings. Prog Org Coatings 63:72–78. doi:10.1016/j.porgcoat.2008.04.008
18. Brown EN, Kessler MR, Sottos NR, White SR (2003) In situ poly(urea–formaldehyde) microencapsulation of dicyclopentadiene. J Microencapsul 20:719–730. doi:10.1080/0265204031000154160
19. Gragert M, Schunack M, Binder WH (2011) Azide/alkyne-"Click"-reactions of encapsulated reagents: toward self-healing materials. Macromol Rapid Commun 32:419–425. doi:10.1002/marc.201000687
20. Patchan MW, Baird LM, Rhim YR, LaBarre ED, Maisano AJ, Deacon RM, Xia Z, Benkoski JJ (2012) Liquid-filled metal microcapsules. ACS Appl Mater Interfaces 4:2406–2412. doi:10.1021/am201861j
21. Brochu ABW, Chyan WJ, Reichert WM (2012) Microencapsulation of 2-octylcyanoacrylate tissue adhesive for self-healing acrylic bone cement. J Biomed Mater Res Part B Appl Biomater 100B:1764–1772. doi:10.1002/jbm.b.32743
22. Li C, Tan J, Li H, Yin D, Gu J, Zhang B, Zhang Q (2015) Thiol-isocyanate click reaction in a Pickering emulsion: a rapid and efficient route to encapsulation of healing agents. Polym Chem 6:7100–7111. doi:10.1039/C5PY01323B
23. Li J, Hitchcock AP, Stöver HDH (2010) Pickering emulsion templated interfacial atom transfer radical polymerization for microencapsulation. Langmuir 26:17926–17935. doi:10.1021/la102867v
24. Yang Y, Ning Y, Wang C, Tong Z (2013) Capsule clusters fabricated by polymerization based on capsule-in-water-in-oil Pickering emulsions. Polym Chem 4:5407–5415. doi:10.1039/c3py00620d
25. Van Den Dungen ETA, Klumperman B (2010) Synthesis of liquid-filled nanocapsules via the miniemulsion technique. J Polym Sci Part A Polym Chem 48:5215–5230. doi:10.1002/pola.24322
26. Van den Dungen ETA, Klumperman B (2010) Self healing composition (Stichting Dutch Polymer Institute), WO2010081713
27. Jackson AC, Bartelt JA, Marczewski K, Sottos NR, Braun PV (2011) Silica-protected micron and sub-micron capsules and particles for self-healing at the microscale. Macromol Rapid Commun 32:82–87. doi:10.1002/marc.201000468
28. Zhao Y, Fickert J, Landfester K, Crespy D (2012) Encapsulation of self-healing agents in polymer nanocapsules. Small 8:2954–2958. doi:10.1002/smll.201200530
29. Galgali G, Schlangen E, Van Der Zwaag S (2011) Synthesis and characterization of silica microcapsules using a sustainable solvent system template. Mater Res Bull 46:2445–2449. doi:10.1016/j.materresbull.2011.08.028
30. Yang Z, Hollar J, He X, Shi X (2011) A self-healing cementitious composite using oil core/silica gel shell microcapsules. Cem Concr Compos 33:506–512. doi:10.1016/j.cemconcomp.2011.01.010
31. Di Credico B, Levi M, Turri S (2013) An efficient method for the output of new self-repairing materials through a reactive isocyanate encapsulation. Eur Polym J 49:2467–2476. doi:10.1016/j.eurpolymj.2013.02.006
32. Strzelec K, Leśniak E, Janowska G (2005) New polythiourethane hardeners for epoxy resins. Polym Int 54:1337–1344. doi:10.1002/pi.1861
33. Strzelec K, Baczek N, Ostrowska S, Wasikowska K, Szynkowska MI, Grams J (2012) Synthesis and characterization of novel polythiourethane hardeners for epoxy resins. Comptes Rendus Chim 15:1065–1071. doi:10.1016/j.crci.2012.09.003
34. Gumula T, Szatkowski P (2016) Regeneration efficiency of composites containing two-sized capillaries. Polym Compos 37:1223–1230. doi:10.1002/pc.23287
35. ISO 178:2010(E) (2010) Plastics—determination of flexural properties
36. Prajer M, Wu X, Garcia SJ, van der Zwaag S (2015) Direct and indirect observation of multiple local healing events in successively loaded fibre reinforced polymer model composites using healing agent-filled compartmented fibres. Compos Sci Technol 106:127–133. doi:10.1016/j.compscitech.2014.11.013

37. Grein A, da Silva BC, Wendel CF, Tischer CA, Sierakowski MR, Moura ABD, Iacomini M, Gorin PAJ, Simas-Tosin FF, Riegel-Vidotti IC (2013) Structural characterization and emulsifying properties of polysaccharides of *Acacia mearnsii* de Wild gum. Carbohyd Polym 92:312–320. doi:10.1016/j.carbpol.2012.09.041
38. Shackle DR, Cousin MJ, Pack GD (1985) Method for producing microcapsules by interfacial photopolymerization and microcapsules formed thereby U.S. Patent 4,532,183
39. Wool RP, O'Connor KM (1981) A theory of crack healing in polymers. J Appl Phys 52:5953–5963. doi:10.1063/1.328526
40. Mattioda G, Obellianne P, Gauthier H, Loiseau G, Millischer R, Donadieu A, Mestre M (1975) Synthesis and pharmacological properties of 4-piperazino-5-methylthiopyrimidines. selection of new antiemetic agents. J Med Chem 18:553–559
41. Song L, Ye Q, Ge X, Misra A, Tamerler C, Spencer P (2016) Self-strengthening hybrid dental adhesive via visible-light irradiation triple polymerization. RSC Adv 6:52434–52447. doi:10.1039/C6RA09933E
42. Pereira FS, Da Silva Agostini DL, Job AE, González ERP (2013) Thermal studies of chitin–chitosan derivatives. J Therm Anal Calorim 114:321–327. doi:10.1007/s10973-012-2835-z